Integrative and Comparative Biology Advance Access published May 6, 2008

Hydrodynamic flow control in marine mammals

Frank E. Fish,[1,*] Laurens E. Howle[†] and Mark M. Murray[§]

[*]Department of Biology, West Chester University, West Chester, PA 19383, USA; [†]Mechanical Engineering and Material Science Department and Center for Nonlinear and Complex Systems, Duke University, Durham, NC 27708-0300, USA; [§]Mechanical Engineering Department, United States Naval Academy, Annapolis, MD 21402, USA

Synopsis The ability to control the flow of water around the body dictates the performance of marine mammals in the aquatic environment. Morphological specializations of marine mammals afford mechanisms for passive flow control. Aside from the design of the body, which minimizes drag, the morphology of the appendages provides hydrodynamic advantages with respect to drag, lift, thrust, and stall. The flukes of cetaceans and sirenians and flippers of pinnipeds possess geometries with flexibility, which enhance thrust production for high efficiency swimming. The pectoral flippers provide hydrodynamic lift for maneuvering. The design of the flippers is constrained by performance associated with stall. Delay of stall can be accomplished passively by modification of the flipper leading edge. Such a design is exhibited by the leading edge tubercles on the flippers of humpback whales (*Megaptera novaeangliae*). These novel morphological structures induce a spanwise flow field of separated vortices alternating with regions of accelerated flow. The coupled flow regions maintain areas of attached flow and delay stall to high angles of attack. The delay of stall permits enhanced turning performance with respect to both agility and maneuverability. The morphological features of marine mammals for flow control can be utilized in the biomimetic design of engineered structures for increased power production and increased efficiency.

Introduction

The laws of momentum, energy, and mass conservation dictate that locomotion by animals is an energy demanding activity. Movement through water requires the transfer of momentum from the animal to the aquatic environment. The energetic consequences of this transfer are compounded as the fluid medium is relatively dense with a high viscosity and incurs large energy losses from turbulent, viscous flow. Although energy is always lost in overcoming the drag on the body and the production of thrust to move forward, reduction of such erratic flow (eddies, turbulence, boundary layer separation) about a swimming animal limits even greater energy losses to the water. As these energy losses determine the performance of the animal (i.e., speed, acceleration, maneuverability), control of flow affects an animal's survival and is potentially subject to strong evolutionary selection pressures (Daniel and Webb 1987).

Marine mammals (e.g., cetaceans, pinnipeds, and sirenians) are far removed from their terrestrial ancestors and as such are specialized to live and forage in water, having adapted to the aquatic environment (Howell 1930). Many of these animals migrate long distances and are apex predators that are characterized as high-speed swimmers (Lang 1975; Feldkamp, 1987; Fish et al. 1988; Fish and Hui 1991; Fish and Rohr 1999; Rohr et al. 2002). The evolution of aquatic habits in marine mammals necessitated the evolution of adaptations that allowed these mammals to optimize energy use by reduction of resistive forces and increased propulsive force production and efficiency (Fish 1996; Williams 1998). Key to these hydrodynamic improvements has been the control of flow.

Water flow can be manipulated around the body and appendages both actively and passively (Fish and Lauder 2006). Active flow control mechanisms use movement of the propulsive appendages and activation of body musculature to modify the wake flow structure. Vorticity shed from the body or appendages as structured vortices or shear layers is utilized to vector hydrodynamic forces during propulsion, maneuvering, and trim control. Passive mechanisms rely on structural and morphological components of the body, which dictate flow over the body surface.

This article will focus on mechanisms involved with active and passive flow control in marine

From the symposium "Going with the Flow: Ecomorphological Variation across Aquatic Flow Regimes" presented at the annual meeting of the Society for Integrative and Comparative Biology, January 2–6, 2007, at San Antonio, Texas.

[1]E-mail: ffish@wcupa.edu

Integrative and Comparative Biology, pp. 1–13
doi:10.1093/icb/icn029

Report Documentation Page

Form Approved
OMB No. 0704-0188

1. REPORT DATE	2. REPORT TYPE	3. DATES COVERED
MAY 2008		**00-00-2008 to 00-00-2008**

4. TITLE AND SUBTITLE	5a. CONTRACT NUMBER
Hydrodynamic flow control in marine mammals	5b. GRANT NUMBER
	5c. PROGRAM ELEMENT NUMBER
6. AUTHOR(S)	5d. PROJECT NUMBER
	5e. TASK NUMBER
	5f. WORK UNIT NUMBER
7. PERFORMING ORGANIZATION NAME(S) AND ADDRESS(ES) **West Chester University ,Department of Biology,West Chester,PA,19383**	8. PERFORMING ORGANIZATION REPORT NUMBER
9. SPONSORING/MONITORING AGENCY NAME(S) AND ADDRESS(ES)	10. SPONSOR/MONITOR'S ACRONYM(S)
	11. SPONSOR/MONITOR'S REPORT NUMBER(S)

12. DISTRIBUTION/AVAILABILITY STATEMENT
Approved for public release; distribution unlimited

13. SUPPLEMENTARY NOTES

14. ABSTRACT

15. SUBJECT TERMS

16. SECURITY CLASSIFICATION OF:			17. LIMITATION OF ABSTRACT	18. NUMBER OF PAGES	19a. NAME OF RESPONSIBLE PERSON
a. REPORT	b. ABSTRACT	c. THIS PAGE			
unclassified	**unclassified**	**unclassified**	**Same as Report (SAR)**	**13**	

mammals. The report is not a comprehensive review of all mechanisms. Specific examples of flow control will be examined in which improved experimental techniques from engineering and medicine were used. These techniques have elucidated evolutionarily novel, morphological adaptations for flow control in marine mammals that have technological application through the biomimetic approach (Triantafyllou and Triantafyllou 1995; Taubes 2000; Anderson and Kerrebrock 2002; Bandyopadhyay 2004; Fish 2006a).

Active flow control

Aquatic animals that swim using body and caudal fin (BCF) undulations pass a travelling wave of increasing amplitude posteriorly along the body (Lindsey 1978). The movements of the animal interact with the water in the generation of controlled body-bound vorticity (Wolfgang et al. 1999). The vorticity is smoothly propagated along the flexing body toward the tail. This vorticity is eventually shed at the trailing edge of the tail producing vortices of alternating-sign in the wake (i.e., reverse Karman street) in the production of a thrust jet (Weihs 1972). For BCF swimmers, the propulsive wave may be produced over different lengths of the body. BCF undulators are characterized along a continuum as anguilliform, subcarangiform, carangiform or thunniform, where the propulsive wave is confined more posteriorly, respectively (Breder 1926; Webb 1975; Lindsey, 1978). This undulatory continuum has functional implications. Thunniform swimmers, such as cetaceans, are characterized as high speed, high efficiency swimmers; whereas, lower swimming performance is associated with anguilliform and subcarangiform swimmers, such as the manatee (*Trichechus manatus*) (Webb 1975; Webb 1978; Fish and Rohr 1999; Kojeszewski and Fish 2007).

Flexible propulsors

In the thunniform mode, propulsive thrust production is confined to oscillations of the caudal hydrofoil (Lighthill 1969; Webb 1975). The propulsive hydrofoils of cetaceans, flukes, are lateral extensions of the distal tail. Structurally, the flukes are composed of fibrous connective tissue (Felts 1966). Biomechanically, the flukes act like a pair of oscillating wings (Vogel 1994). Thrust is generated as a component of an anteriorly directed lift force as the flukes are vertically oscillated (Fish 1998a, 1998b). Despite the importance of the flukes as the sole propulsive device, there has been limited research into the interaction of the anatomical design of flukes and their operation.

The hydrodynamic models, which were used to estimate thrust production and propulsive efficiency, considered the flukes as rigid hydrofoils (Parry 1949; Wu 1971; Lighthill 1975; Chopra and Kambe 1977; Fish 1993a, 1993b; 1998a; Liu and Bose 1993). These models did not account for the flexibility of the flukes, but instead considered them rigid structures. The structural components of the flukes (i.e., collagen fibers) are not rigid and permit bending along the axes of both the chord and span (Felts 1966; Curren et al. 1994; Romanenko 2002; Fish et al. 2006a). As structural and kinematic parameters determine locomotor performance, the flexible components of the dolphin flukes in conjunction with its propulsive oscillations are expected to enhance efficiency and energy economy (Alexander 1988; Pabst 1996; Katz and Weihs 1978; Bose 1995; Taylor et al. 2007).

The flukes of cetaceans have been calculated to operate with high propulsive efficiency of 0.75–0.90 (Fish 1998b). This high efficiency surpasses the performance of propellers used in commercial ships, which have maximum efficiencies of 0.70 (Triantafyllou and Triantafyllou 1995). Furthermore, cetaceans are able to adjust thrust production and efficiency by controlling the angle of attack of the oscillating flukes (Long et al. 1997; Fish 1998a, 1998b). The angle of attack is defined as the angle between the tangent of the fluke's path and the axis of the fluke's chord. Maintenance of a positive angle of attack ensures thrust generation throughout the majority of the stroke cycle.

Rotating the flukes about a pitching axis allows for control of angle of attack. The rotation occurs at the base of the flukes, where there is a transition in the caudal vertebrae of the skeleton (Long et al. 1997; Fish 1998b). As the angle of attack is increased, lift will increase faster than the drag for a hydrofoil up to a critical level. Further increase of the angle of attack leads to stall with an increase in drag and precipitous loss of lift. Foils similar to cetacean flukes under steady flow conditions stall at angles of attack over 20°. However, an oscillating high aspect ratio fin can continue to generate lift, and thus thrust, up to an attack angle of 30° (Triantafyllou and Triantafyllou 1995). Stall can be caused by boundary layer separation from the foil surface by either unfavorable pressure gradients or from the formation of vapor bubbles due to cavitation (Iosilevskii and Weihs 2007). Conversely, at the top and bottom of the stroke, the flukes will have zero angle of attack as they rotate through the pitch axis and reverse direction. At these extreme positions, the flukes would be feathered (i.e., chord line parallel to the

incident flow) and have a zero angle of attack. If the flukes were straight and rigid during the vertical change in direction, there would be a period in which no thrust was generated and efficiency was reduced.

Medical computer tomography (CT) scans were made on isolated flukes to access three-dimensional changes in fluke structure due to bending (Fish et al. 2006a). Bending of the flukes changed the three-dimensional geometry of these structures and provided a shape, which potentially enhances propulsion. Flukes are flexible structures that permit chordwise (i.e., direction of leading to trailing edges) bending. When no external load is provided, the flukes have symmetrical cross-sections along the span. When statically bent, the flukes show varying degrees of cambering along the span. Camber is most extreme near the root and decreases toward the fluke tip. However, this camber is negative or opposite what is seen on manufactured wings. For example, the trailing edge bends away from rather than toward the oncoming flow.

The flukes of a swimming white-sided dolphin (*Lagenorhynchus acutus*) showed 35% and 13% deflections across the chord and tip-to-tip span, respectively (Curren et al. 1994). However, a swimming harbor porpoise (*Phocoena phocoena*) displayed almost no bending at either the fluke tips or the trailing edge (Curren et al. 1994). When CT scans of bent flukes were analyzed, camber was evident in both species (Fish et al. 2006a). The flukes of *P. phocoena* exhibited 0.6–3.6% and 3.1–4.3% less cambering than *L. acutus* when bent at 45° and 90°, respectively.

Flexibility across the chord can increase propulsive efficiency (Katz and Weihs 1978, 1979; Bose and Lien 1989; Prempraneerach et al. 2003). Chordwise flexibility increases leading edge suction (Katz and Weihs 1978), which adds to the thrust component of lift. A flexible foil can be cambered dynamically in accordance to local flow conditions (Liao 2004). Thus, cambering provides a favorable orientation of the foil to the incident flow in a time-dependent manner. Chordwise flexibility can increase efficiency by 20% with a small decrease in thrust, compared to a rigid propulsor executing similar oscillations (Katz and Weihs 1978).

Propulsive efficiency for flexible foils reaches a maximum value for a range of Strouhal number ($St = Af/U$, where A is the peak-to-peak vertical displacement of the fluke tip, f is the fluke beat frequency, U is swimming speed) of 0.2–0.35 (Prempraneerach et al. 2003). This range of Strouhal number is in good agreement with the range for swimming cetaceans (Rohr and Fish, 2004). The maximum propulsive efficiency for cetaceans occurs at Strouhal numbers between 0.25 and 0.35 (Rohr and Fishs 2004).

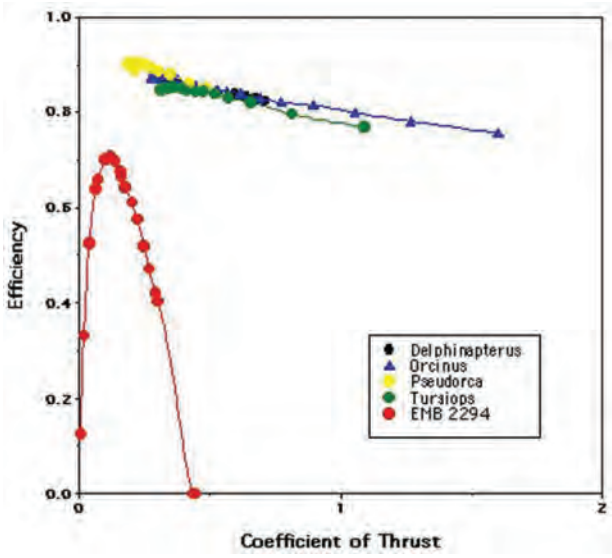

Fig. 1 Comparison of relationships of propulsive efficiency and thrust coefficient for four species of small cetaceans and a typical marine propeller. Data for the whales were obtained from Fish (1998a, b) and data for the propeller (EMB 2294) were from Saunders (1957).

The performance of rigid propellers is limited by the speed and frequency of movement. Standard rotation propellers, such as those found on boats, have a very limited range of operational speeds where efficiency is maximum (Fish and Lauder 2006). Above and below that optimal speed, efficiency falls off precipitously (Breslin and Andersen 1994). The oscillating flukes of cetaceans, however, maintain a high efficiency of operation over a wide range of speeds without any sudden decrease in efficiency (Fig. 1; Fish and Lauder 2006).

Cambering could provide increased lift and thrust production throughout the entire stroke cycle. Cambering would potentially allow the flukes to maintain thrust production through the change in oscillation direction. A smoother transition due to flexibility may allow the flukes to operate without stalling. Curvature of the flukes increases more at the lowermost position of the downstroke compared the middle of the stroke (Romanenko 2002; Fish et al. 2006a). However, increased chordwise flexibility may subject the flukes and the speed of the animal to limitations. There is an upper limit in swimming speed of 10–15 m/s for dolphins, because of the increased leading edge suction and the possibility of stall through cavitation due to flexibility (Iosilevskii and Weihs 2007).

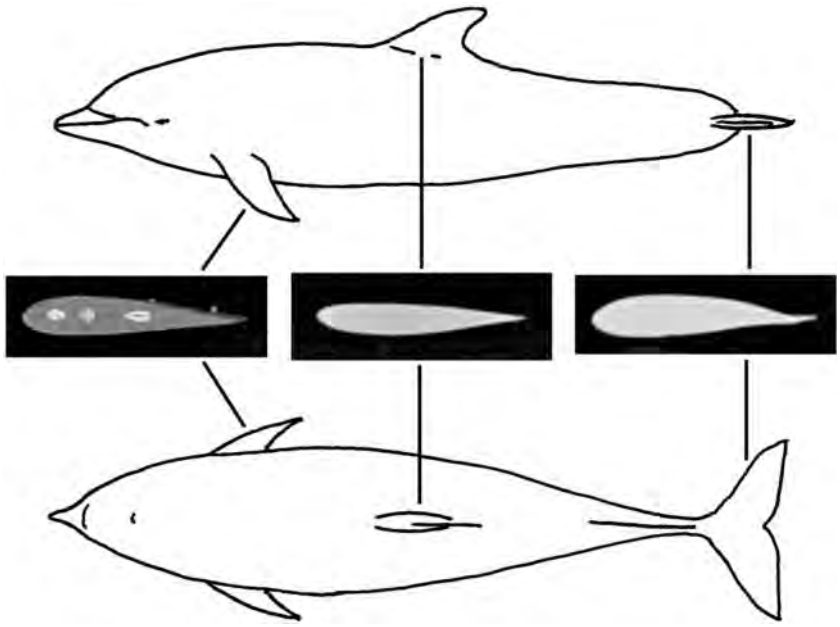

Fig. 2 Streamlining in body and control surfaces of a dolphin. Images of cross-sections of flipper, dorsal fin, and flukes were obtained from CT scans.

Passive flow control

The passive mechanisms of flow control rely on the structural and morphological components of the body (Fish and Lauder 2006).

Streamlining

Drag is minimized primarily by streamlining the shape of the body and the appendages (Webb 1975; Fish 2006b). The streamlined profile of these structures has a fusiform design resembling an elongate teardrop with a rounded leading edge extending to a maximum thickness and a slowly tapering tail. This shape was first investigated in the dolphin by Sir George Cayley (circa 1800) as a solid of least resistance design. Marine mammals display a streamlined, fusiform design. This fusiform shape is sculpted by the distribution of blubber and/or fur covering the body. In addition, the appendages, such as the flukes, flippers, and dorsal fin, have a cross-sectional shape with a fusiform design similar to conventional aircraft wings and hydrofoils (Fig. 2).

Streamlining minimizes drag by reducing the magnitude of the pressure difference over the body (Fish and Hui 1991). This reduced pressure difference allows water in the boundary layer to flow without separation from the body surface until near the trailing edge. As separation occurs, a wake is generated downstream. The wake behind the body is narrow, indicating little distortion to the flow and a small pressure drag. Premature separation of the boundary layer occurs because of instabilities in the flow. A laminar boundary flow is inherently less stable and more prone to premature separation than turbulent flow. An animal may pay a higher energetic cost in frictional drag by allowing the development of a turbulent boundary layer, but the pressure and total drags will be substantially lower than with laminar flow where separation transpires (Webb 1975). It is the delay or prevention of boundary layer separation fostered by streamlining that paramount in minimizing drag. While the idea of a special drag reduction mechanism by maintenance of laminar flow over the bodies of marine mammals has been irresistible (i.e., Gray's paradox; Gray 1936), direct evidence of its existence has been elusive. To date, no conclusive evidence has been found of laminar boundary flow over the entire body surface of fast swimming dolphins (Lang and Daybell 1963; Lang 1966; Webb 1975; Aleyev 1977; Fish and Hui 1991; Fish and Rohr 1999; Fish 2006b; Pavlov 2006).

An indicator of the degree of streamlining is the fineness ratio (FR = body length/maximum diameter). The FR value of 4.5 is considered to provide the least drag for the maximum volume (Fig. 3; von Mises 1945; Hertel 1966; Webb 1975). This conclusion was based on the geometry of a C-Class airship (von Mises 1945). Although pinnipeds and sirenians display body profiles spanning the FR of 4.5, the sea otter (*Enhydra lutris*) and many cetaceans

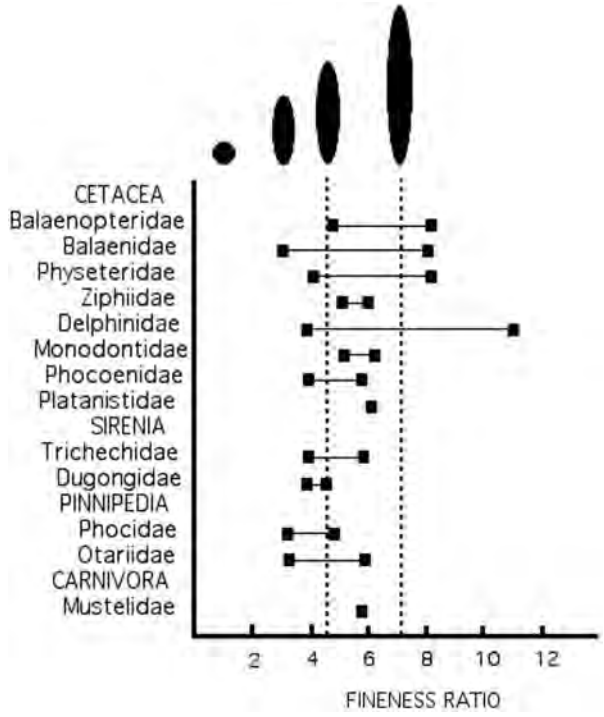

Fig. 3 Comparison of ranges of *FR* for various marine mammal families. The dashed lines indicate *FR* of 4.5 and 7.0, where minimum drag is expected according to von Mises (1945) and Gertler (1950), respectively. Silhouettes show the difference in shape in reference to *FR* from a circular shape (*FR* = 1) to an elongate form (*FR* = 7).

possess body shapes with higher *FR* values (Fig. 3). The high *FR* of the sea otter is most likely a phylogenetic constraint as other members of the Mustelidae have an elongate body (Brown and Lasiewski 1972). The skewing of the body of cetaceans toward higher *FR* values may reflect drag reduction associated with high-speed swimming and large body size. Gertler (1950) demonstrated minimum submerged drag and power requirements at *FR* of 7 for streamlined bodies of revolution with the application to the design of high-speed submarines. The models used were 2.7 m long and tested up to 11.3 m/s, which encompasses the swimming speeds of cetaceans (Fish and Rohr 1999).

The variation in *FR* for marine mammals may be tied to the swimming performance associated with each species. Rectilinear swimming and maneuverability have influence on the body morphology (Fish 2002; Woodward et al. 2006). Short bodies with low *FR* may be more suited to slower speed swimming, whereas, elongate bodies may perform better in rapid swimming and maneuvering. Spinner dolphins (*Stenella longirostris*) have a higher *FR* than similarly sized dolphins, which reduces their second moment of area and allows them to perform spinning aerial maneuvers with greater ease (Fish et al. 2006b).

FR is however a crude indicator of the streamlining of the body, because it does not provide information on changes in body contour. Another indicator of body streamlining is the position of the maximum thickness, called the shoulder. Shoulder position is important because this is where transition from laminar to turbulent flow and boundary layer separation are likely to occur. Anterior of the shoulder, the pressure distribution favors maintenance of a laminar boundary layer. The position of the shoulder in the most rapidly swimming aquatic mammals is displaced posteriorly which is similar to engineered wings with ''laminar'' profiles, which reduce drag through maintenance of laminar boundary flow.

For dolphins, the shoulder position is 34–45% of the body length from the beak (Fish and Rohr 1999). Experiments on flow visualization using a fluorescent dye applied to a dolphin's melon showed the flow to be laminar over the anterior 32% of the dolphin. Transition began before the dorsal fin with turbulence aft of the fin. Separation of the boundary flow occurred smoothly near the base of the flukes. Flow visualization using bioluminescence within the boundary layer of dolphins and seals similarly indicated a lack of separation from the body surface (Rohr et al. 1998). Flow separation is restricted to the tips of the flukes, flippers, and dorsal fin. The flow separation has been observed as bioluminescent ''contrails''.

The shoulder position is located at 40% of body length for otariid seals and 50–60% of body length for phocid seals from the nose (Fish 1993a, 1993b). The position can be varied in pinnipeds, because the neck is capable of being retracted and extended. Extension of the neck during rapid swimming could modify the flow over the anterior of the seal and reduce drag by extending the region of laminar flow. Such a drag reduction could aid seals in catching fast swimming, elusive prey.

The naked skin of cetaceans is regarded as a means to maintain a smooth flow with an attached boundary layer over the surface of the body. In addition, the cells of epidermis are produced rapidly, which promotes a high rate of skin sloughing (Fish and Rohr 1999). This increased skin sloughing deters organisms, such as barnacles, from attaching to the skin and thus minimizes drag (Fish and Hui, 1991). The properties of the hair of aquatic mammals are noted to reduce drag by aiding in streamlining of the body. The lack of arrector pili muscles in seals and sea otter permits the pelage to lie flat in water minimizing resistance to swimming.

Bumpy surfaces

A smooth, contoured surface is considered the optimal configuration to passively control flow and reduce drag by maintaining laminar flow. However, irregularities in the surface geometry of aquatic organisms can improve performance. Tripping of the boundary layer from laminar to turbulent flow can prevent premature separation with its concomitant increase in drag (Moin and Kim 1997). Microgrooves (riblets) found on the scales of sharks modify the flow regime to reduce drag by 7–8% (Walsh 1990; Bushnell and Moore 1991). Bumps are observed on the surface of various projections (i.e., vibrissae, fin, and flippers) from the body of marine mammals, which similarly may improve hydrodynamic performance (Bushnell and Moore 1991).

Seal vibrissae

While flow control has been associated with increasing locomotor performance in marine mammals, the geometry of particular sensory structures may also use a passive mechanism of flow control. The vibrissae of phocid seals have an ellipsoidal cross-section with regularly repeating sequence of constrictions or wavy profile along its length (Fig. 4; Dehnhardt and Kaminski 1995). Such non-axisymmetrical vibrissal hair shafts suggest potential hydrodynamic properties for seals swimming (Marshall, C. D., personal communication). The beading may decrease drag by acting as vortex generators (Bearman and Owen 1998; Owen et al. 2000). Decreased drag on the vibrissae could aid in detection of stimuli by noise cancellation. Normally, a cylindrical body in a flow will produce a series of alternating vortices in its wake, known as the Kármán vortex street (Prandtl and Tietjens 1934). The alternating nature of the shedding vortices induces vibrations of a cylinder. A cylinder bent sinusoidally generates paired rather than alternating vortices (Owen et al. 2000). Paired vortices could reduce vibrations from water flow over the vibrissae and increase the sensitivity of the vibrissae to detect vibrations and flow irregularities in the environment.

The vibrissae of harbor seals (*Phoca vitulina*) are able to detect vibrations between 5 and 1000 Hz (Renouf 1979). Vibrations that displace the seal's vibrissae by $<1\,\mu m$ were perceptible at 1000 Hz, although there is less sensitivity at lower frequencies. A harbor seal could detect a water velocity of 245 μm/s, which is considered several orders of magnitude lower than the velocity of water flow in the wake of a swimming fish (Dehnhardt et al. 1998). Dehnhardt et al. (1998) argued that the vibrissae

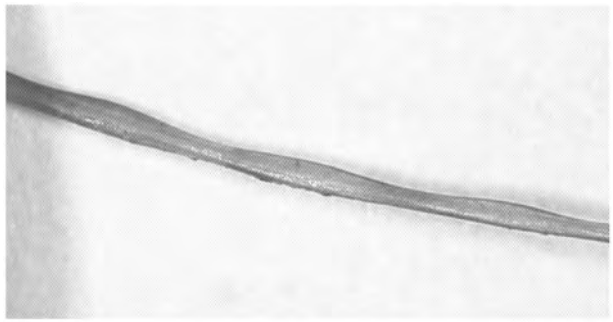

Fig. 4 Photomicrograph of phocid vibrissae from a harp seal (*Pagophilus groenlandicus*), showing bumps along the length.

are a hydrodynamic receptor system tuned to the frequency range of fish-generated water movements. The hydrodynamic trails produced by a swimming fish are long lasting and could be detected by phocid seals (Hanke et al. 2000; Dehnhardt et al. 2001).

Cetacean tubercles

In certain instances, the normally smooth skin of cetaceans has bumpy projections. Small bumps are observed in discrete locations on the bodies of porpoises (family Phocoenidae). The finless porpoise (*Neophocaena phocaenoides*) has small wart-like excrescences on its back to carry young out of the water (Pilleri and Peixun 1979). Small rounded tubercles of about 1 mm are located along the leading edge of the dorsal fin of porpoises (*Phocoena* sp.) (Ridgway and Harrison 1999; Evans et al. 2001). The position of the tubercles allude to a possible hydrodynamic function in turbulizing the water flow to modify the tip vortex shed from the dorsal fin, although this effect has not be investigated.

The humpback whale (*Megaptera novaeangliae*) flipper has large protuberances or tubercles located on the leading edge (Fig. 5), which gives this surface a scalloped appearance (Winn and Reichley 1985). The flipper planform is elliptical with a high aspect ratio (span/chord) and tapered distally. Locations of the tubercles correspond to the positions of the cartilages of the manus (Tomilin 1957; Edel and Winn 1978; True 1983). From 10 to 11 tubercles are found along the leading edge of the flipper (Fig. 5). The tubercles are confined to the distal and medial segments of the flipper. The most proximal tubercle is located at 30% of the flipper span (Fish and Battle 1995). The smallest is located near the flipper tip. Intertubercular distances decrease distally, although intertubercular distances remains relatively constant at 7–9% of span over the mid-span of the flipper (Fig. 6).

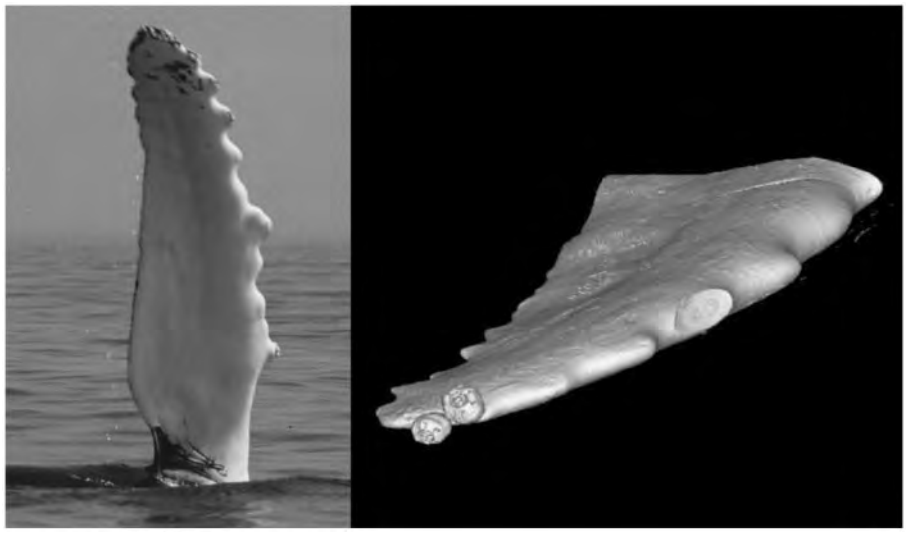

Fig. 5 Humpback whale (*M. novaeangliae*) flipper. Detail views of pectoral flipper showing leading edge tubercles (left; courtesy of W.W. Rossiter) and three-dimensional reconstruction of flipper tip from CT scans (right).

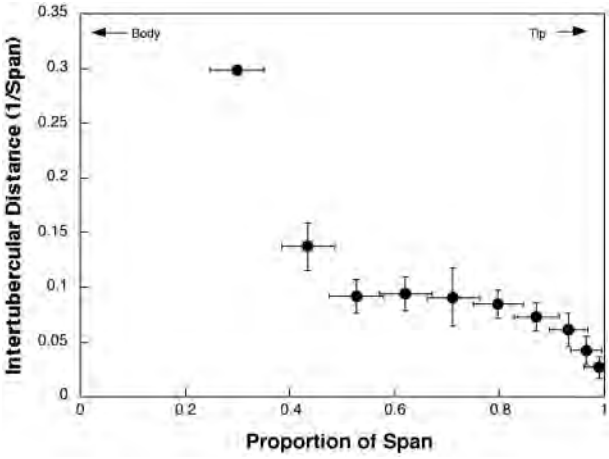

Fig. 6 The mean distances (±SD) between centers of adjacent tubercles (intertubercle distance) is expressed as the mean positions of the tubercles as a proportion of total flipper span (±SD) from image of 77 humpback whale flippers.

The tubercles found along the leading edge of the flippers of the humpback whale can have a hydrodynamic effect. The position and number of tubercles on the flipper suggested analogues with specialized leading edge control devices associated with improvements in hydrodynamic performance. Bushnell and Moore (1991) suggested that humpback tubercles reduce drag due to lift on the flipper. The occurrence of ''morphological complexities'' on a lifting body could reduce, or use, pressure variation at the tip to decrease drag and improve lift to prevent tip stall. In addition, leading edge control devices can maintain lift and avoid stall at high attack angles and low speeds (Hoerner 1965).

Experiments on wavy bluff bodies showed periodic variation in the wake width across the span (Owen et al 2000). A wide wake occurred where the body protruded downstream and a narrow wake occurred where the body protruded upstream. Drag reduction of at least 30% was achieved on a wavy bluff body compared to equivalent straight bodies (Bearman and Owen 1998). Flow visualization experiments conducted on a model wing section with leading edge tubercles similar to those on humpback flippers showed that vorticity was produced (Johari et al. 2007).

The tubercles of the humpback whale flipper function to generate vortices by excitation of flow to maintain lift and prevent stall at high angles of attack (Wu et al. 1991; Miklosovic et al. 2004; Fish and Lauder 2006). The function of the tubercles may be analogous to strakes used on aircraft or as small, multiple delta wings. Both strakes and delta wings are large vortex generators that change the stall characteristics of a wing (Hoerner 1965; Hurt 1965). Stall is postponed because the vortices exchange momentum within the boundary layer to keep it attached over the wing surface. Lift is maintained at higher angles of attack compared to straight wings or wings without strakes, although maximum lift is not increased.

Comparisons of wing sections with and without tubercles using computational fluid dynamic (CFD) models demonstrated differing flow patterns affecting hydrodynamic performance. A panel method showed a 4.8% increase in lift, a 10.9% reduction in induced drag, and a 17.6% increase in lift to drag ratio for wing sections with tubercles at 10° angle of attack (Watts and Fish 2001). A general purpose

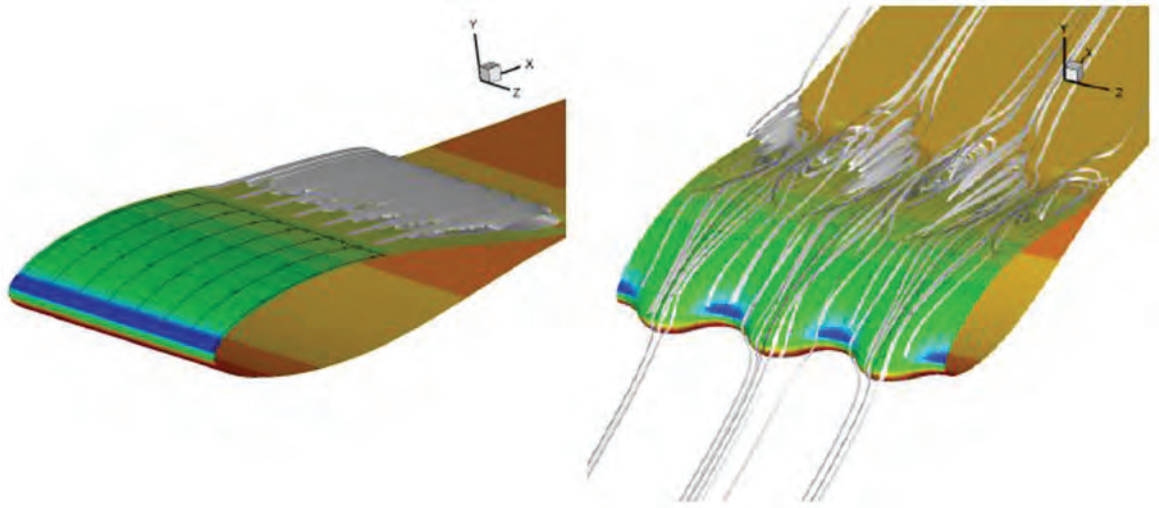

Fig. 7 Pressure contours and particle path lines at $\alpha = 10^{\circ}$ for NACA 63-021 with straight leading edge (left) and with tubercles (right). An unsteady Reynolds–Averaged Navier–Stokes (RANS) simulation was used. A separation line is shown on the wing section without tubercles. For the wing with tubercles, large vortices are formed posterior of the troughs along the leading edge and flow posterior of the tubercles is shown as straight streamlines without separation. Images courtesy of E. Paterson.

incompressible unsteady Reynolds–Averaged Navier–Strokes (RANS) simulation (CFDSHIP; Paterson et al. 2003) was used to study the effect of tubercles on flow separation and hydrofoil performance for a NACA 63-021 baseline foil. At simulated flow conditions corresponding to a Reynolds number (*Re*) of 1,000,000 ($Re = UL/\nu$, where U is whale swimming speed, L is the foil chord length, and ν is the kinematic viscosity of water). The surface pressure contours and streamlines at a 10° angle of attack, flow separation pattern and surface pressure were dramatically altered by the tubercles (Fig. 7). For regions downstream of tubercle crest, separation was delayed almost to the trailing edge. This was due to an increase in pressure on the suction side, which locally reduced the adverse pressure gradient. This pressure gradient reduced lift in comparison to baseline foil. However, the flow induced by the tubercles delays stall by the wing (Fish and Lauder 2006; van Nierop et al. 2008).

Wind tunnel experiments provided evidence that the leading edge tubercles on humpback whale flippers serve to delay stall angle and increase total lift without significantly increasing drag (Miklosovic et al. 2004). Idealized 1/4 scale models similar to a humpback whale flipper with and without tubercles were machined from polycarbonate. Model flippers were based on a NACA 0020 section. The first model flipper had a smooth leading edge, while the second model had a sinusoidal (scalloped) leading edge profile approximating the pattern of tubercles found on the humpback whale flipper. The scalloped flipper had an intertubercular spacing and size that decreased toward the distal tip.

Tests on the model flippers were performed in a low-speed closed-circuit wind tunnel at atmospheric conditions (Miklosovic et al. 2004). The *Re* was 500,000, which is ~1/2 of the value of the whale at lunge feeding speed (2.6 m/s). The results of the wind tunnel test are shown in Fig. 8. In this figure, the lift coefficient $C_L = 2L(\rho U_\infty{}^2 A)^{-1}$ and drag coefficient $C_D = 2D(\rho U_\infty{}^2 A)^{-1}$ are plotted against the angle of attack, α (Fig 9A, B). The *L/D* ratio, which quantifies the drag cost of producing lift, or aerodynamic efficiency, is shown in Fig. 8c. The experiments show the stall angle occurs at 16.3° for the scalloped case (triangles) as compared to 12° for the unperturbed case (solid line). The maximum lift was shown to be somewhat greater for the scalloped model flipper (Fig. 8a). The drag coefficient for the perturbed geometry is less that of the smooth geometry in the range $12^{\circ} < \alpha < 17^{\circ}$ and is only slightly greater in the range $10^{\circ} < \alpha < 12^{\circ}$ (Fig. 8b). Peak *L/D* is greater for the scalloped geometry (Fig. 8c).

Delayed stall was also found for wind and water tunnel experiments on foil sections, but with reduced lift and increased drag at prestall angles of attack of the baseline foil (Johari et al. 2007; Miklosovic et al. 2007). At poststall angles of attack, the lift could be up to 50% higher than baseline foils (Johari et al. 2007). This higher lift was found to occur with increasing size of the tubercles, whereas the number and distance between tubercles had minor effects on

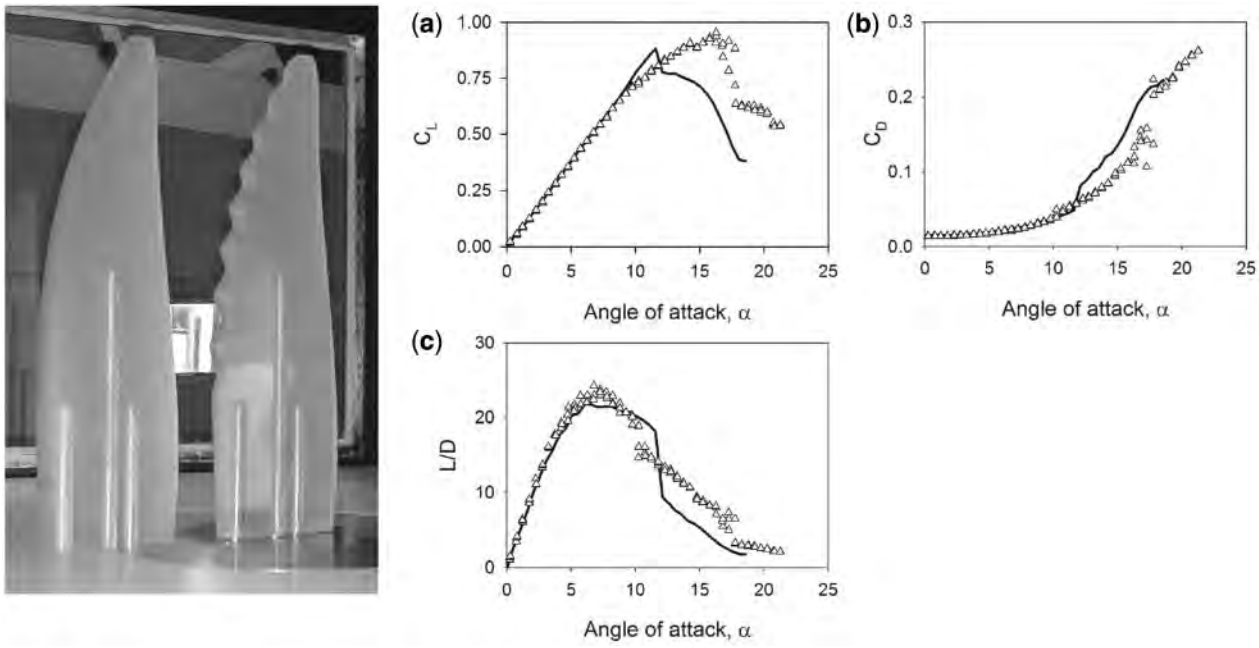

Fig. 8 Humpback whale flipper models and results of wind tunnel experiments. The models (left) with and without tubercles were machined from clear polycarbonate, based on a symmetrical NACA 0020 foil section. Lift and drag data (right) for the flipper models were obtained from tests in a wind tunnel. The solid lines in A, B, and C show the average of the data for the flipper model without tubercles and open triangles are for the model with tubercles. **(a)** Wind tunnel measurements of lift coefficient, C_L, displayed as a function of angle of attack α. The model with the tubercles maintains lift to higher α than the model without tubercles. The effect of the tubercles is to delay stall. **(b)** Drag coefficient, C_D, shows no difference between the models up to $\alpha = 11^\circ$. At higher α, the model with tubercles has a lower C_D than the model without tubercles. **(c)** Aerodynamic efficiency, *L/D*. From Miklosovic et al. (2004).

force production. In addition, when stall did occur for foils with tubercles, the stall was softer than stall for the baseline foil. Although the lift and drag results are counter to the wind tunnel experiments performed by Miklosovic et al. (2004), they indicate that the tubercles improve overall performance only when situated on a full three-dimensional wing rather than a more two-dimensional foil section (Miklosovic et al. 2007).

What is the advantage of having leading edge tubercles on the flippers of humpback whales? Delay of stall and improvements in lift production seem unnecessary to an animal that is near neutrally buoyant in water. The typical feeding behavior of other rorqual whales of the *Balaenopteridae* is to swim rectilinearly with little maneuvering into large shoals of planktonic prey (Ridgway and Harrison 1985; Whitehead and Carlson 1988). However, maneuverability of the humpback whale is associated particularly with their feeding behavior and the whales are highly aquabatic. Despite their large size (up to 14 m and >30 ton), humpback whales can perform underwater somersaults (Jurasz and Jurasz 1979).

Humpback whales feed on patches of plankton or fish schools including euphausiids, herring, and capelin (Jurasz and Jurasz 1979; Winn and Reichley 1985; Dolphin 1988; Pauly et al. 1998). Whales lunge toward their prey at ~2.6 m/s (Jurasz and Jurasz 1979; Hain et al. 1982). The flippers are deployed in "inside loop" behavior when the whale then rolls 180° making a sharp U-turn in 1.5–2 body lengths and lunges toward the prey (Hain et al. 1982). In "bubble netting", underwater exhalations from the blowhole produce bubble clouds or columns, which completely encircle and concentrate the prey (Jurasz and Jurasz 1979; Hain et al. 1982; Winn and Reichley 1985). Bubble nets are produced as the whale swims toward the surface in a circular pattern from a depth of 3–5 m. At completion of the bubble net, the whale pivots with its flippers and banks to the inside as it turns sharply into the center of the net (Hain et al. 1982). Bubble net size varies from a minimum diameter of 1.5 m for corralling euphausiids to a maximum diameter of 50 m to capture herring (Fig. 9; Jurasz and Jurasz 1979).

The unusual length of the pectoral flippers and presence of leading edge tubercles of the humpback whale allow for increased maneuverability (Edel and Winn 1978; Jurasz and Jurasz 1979; Fish and Battle 1995). The flippers act as biological hydroplanes to produce lift to turn. In a banking turn, the body rolls

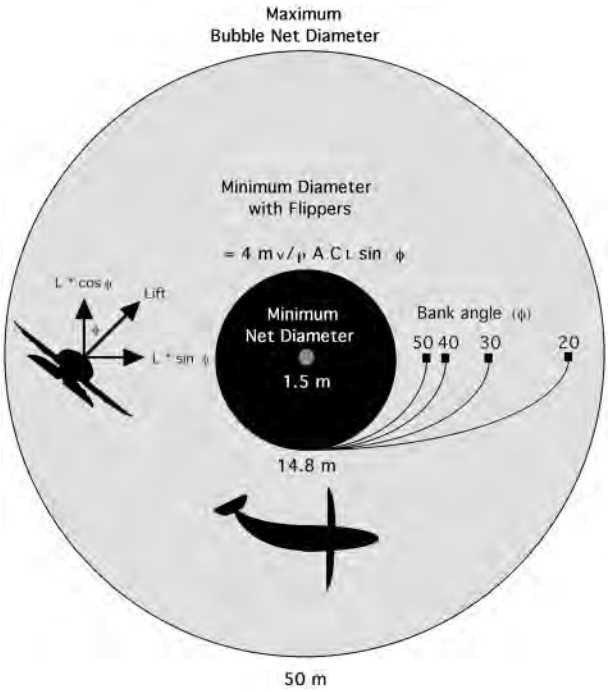

Fig. 9 Calculated and observed turning performance of the humpback whale (*Megaptera novaeangliae*). The calculated minimum turning diameter (14.8 m) for a 9 m whale is shown by the outer margin of the black circle, based on the equation shown. The margins of the turn for various bank angles are shown by curved lines. The minimum and maximum diameters of bubble nets, which were reported in the literature are shown by the margin of the central circle and the outer circle, respectively. The lift (L) vectors with respect to bank angle (ϕ) are illustrated in the inset. Symbols for the equation of the minimum diameter of a turn using flippers are virtual mass of the whale (m_v), density of water (ρ), planar area of both flippers (A), and coefficient of lift (C_L). The silhouette indicates the dimensions of the whale.

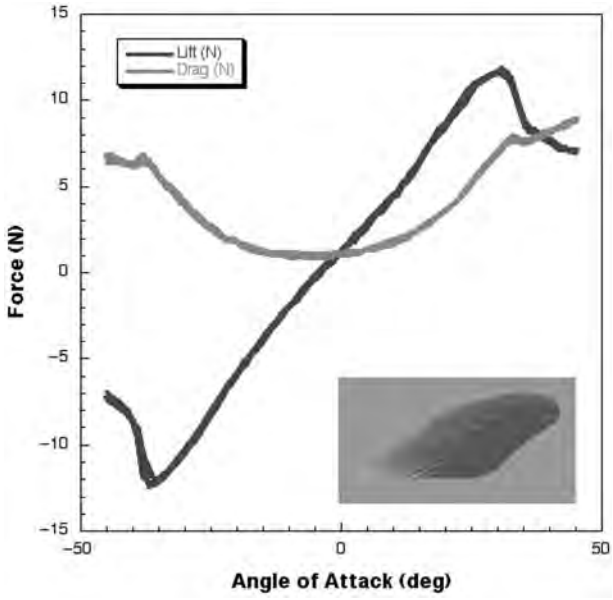

Fig. 10 Example of hydrodynamic results for a model flipper from a harbor porpoise (*P. phocoena*) that was measured in a water tunnel. The lift (black line) and drag (gray line) forces are shown as a function of the angle of attack. The stall, indicated by the severe change in the lift curve, occurs at greater positive and negative angles of attack than conventional wings. The insert shows a three-dimensional rendering of the flipper.

or tilts toward the inside of the turn. The lift force developed by the flippers has a horizontal component that supplies the centripetal force necessary to maintain the turn (Alexander 1983; Weihs 1981, 1993). Lift and bank angle are inversely related to turn radius (Alexander 1983). Lifting bodies used in turning must operate at high angles of attack, while maintaining lift (von Mises 1945; Hurt 1965; Weihs 1993).

Small radius turns are accomplished by increasing the bank angle, which increases the horizontal component of the lift vector (Fig. 9), and/or increasing the angle of attack. However, at too high an angle of attack, the flipper could stall and the whale would travel with a straight trajectory tangent to its original curved path. The action would be analogous to a car contacting a patch of ice while executing a turn. The tubercles act to delay or prevent stall. Without stall, the whale would be able to execute tighter and more rapid turns during feeding maneuvers.

Concluding remarks

The incorporation of novel structures and mechanisms from nature into the design and function of machines is attempted through biomimetics. The goal of biomimetics is to use biological inspiration to engineer machines that emulate the performance of animals (Vogel 1998; Taubes 2000; Fish 2006a) particularly in instances where animal performance exceeds current mechanical technology. An understanding of the hydrodynamic mechanisms by which marine mammals control flow may lead to improved hydrofoil and wing design for engineered devices (Fig. 10). There is a strong possibility that the hydrodynamic results of the work on the marine mammals can be applied in the design of water- and aircraft as these devices function at similar high Reynolds numbers.

Active mechanisms of flow control as exhibited by flexibility of the flukes of cetaceans may provide an alternate or superior solution to propulsion involving rotational or oscillating, engineered propellers (Fish and Rohr 1999; Bandyopadhyay 2004). Passive flow control has advantages of eliminating complex, costly, high maintenance, and heavy control

mechanisms, while improving performance. Demonstration of significant practical applications on delaying of stall, increased lift production and reduced drag is likely to attract considerable attention from aero/hydro-dynamic engineers. For example, the leading edge tubercles of the humpback whale flipper provide a passive means of flow control over a lifting surface, which could be applied to engineered devices. Enhanced maneuverability by the addition of leading edge tubercles has potential application in the development of modern vehicles operating in air or water.

Acknowledgments

We are grateful for the assistance of J. Arruda, S. Cramer, S. Farjo, L. K. Fish, P. Habecker, D. R. Ketten, M. Moore, J. Parsons, B. Schuelkens, and P. Weber. The research in this article was supported by grants from the National Science Foundation (IOS–0640185), the College of Arts and Sciences Support and Development Award, West Chester University to F.E.F., the Office of Naval Research (N00014-02-1-0046 to F.E.F.), and the Defense Advanced Projects Research Agency (W911NF-07-1-0288 to L.E.H.). The research on animals described in this article was performed in accordance with the West Chester University Institutional Animal Care and Use Committee.

References

Aleyev YG. 1977. Nekton. Den Hague (the Netherlands): Junk.

Alexander RMcN. 1983. Animal mechanics. Oxford (UK): Blackwell.

Alexander RMcN. 1988. Elastic mechanisms in animal movement. Cambridge: Cambridge University Press.

Anderson JM, Kerrebrock PA. 2002. Biomimetics in action: design and performance of an autonomous robotic fish. In: Ayers J, Davis JL, Rudolph A, editors. Neurotechnology for biomimetic robots. Cambridge (MA): MIT Press. p. 297–308.

Bandyopadhyay PR. 2004. Trends in biorobotic autonomous undersea vehicles. J Ocean Eng 29:1–32.

Bearman PW, Owen JC. 1998. Reduction of bluff-body drag and suppression of vortex shedding by the introduction of wavy separation lines. J Fluid Struct 12:123–130.

Bose N. 1995. Performance of chordwise flexible oscillating propulsors using a time-domain panel method. Int Shipbuild Progr 42:281–294.

Bose N, Lien J. 1989. Propulsion of a fin whale (*Balaenoptera physalus*): why the fin whale is a fast swimmer. Proc R Soc Lond B 237:175–200.

Breder CM. 1926. The locomotion of fishes. Zoologica 4:159–297.

Breslin JP, Anderson P. 1994. Hydrodynamics of ship propellers. Cambridge: Cambridge University Press.

Brown JH, Lasiewski RC. 1972. Metabolism of weasels: the cost of being long and thin. Ecology 53:939–943.

Bushnell DM, Moore KJ. 1991. Drag reduction in nature. Annu Rev Fluid Mech 23:65–79.

Chopra MG, Kambe T. 1977. Hydrodynamics of lunate-tail swimming propulsion. Part 2. J. Fluid Mech 79:49–69.

Curren KC, Bose N, Lien J. 1994. Swimming kinematics of a harbor porpoise (*Phocoena phocoena*) and an Atlantic white-sided dolphin (*Lagenorhynchus acutus*). Mar Mamm Sci 10:485–492.

Daniel TL, Webb PW. 1987. Physics, design, and locomotor performance. In: Dejours P, Bolis L, Taylor CR, Weibel ER, editors. Comparative physiology: life in water and on land. New York: Liviana Press, Springer. p. 343–369.

Dehnhardt G, Kaminski A. 1995. Sensitivity of the mystacial vibrissae of harbour seals (*Phoca vitulina*) for size differences of actively touched objects. J Exp Biol 198:2317–2323.

Dehnhardt G, Mauck B, Bleckmann H. 1998. Seal whiskers detect water movements. Nature 394:235–236.

Dehnhardt G, Mauck B, Hanke W, Bleckmann H. 2001. Hydrodynamic trail-following in harbor seals (*Phoca vitulina*). Science 293:102–104.

Dolphin WF. 1988. Foraging dive patterns of humpback whales, *Megaptera novaeangliae*, in southeast Alaska: cost-benefit analysis. Can J Zool 66:2432–2441.

Edel RK, Winn HE. 1978. Observations on underwater locomotion and flipper movement of the humpback whale *Megaptera novaeangliae*. Mar Biol 48:279–287.

Evans K, Kemper C, Hill M. 2001. First records of the spectacled porpoise *Phocoena dioptrica* in continental Australian waters. Mar Mamm Sci 17:161–170.

Feldkamp SD. 1987. Swimming in the California sea lion: morphometrics, drag and energetics. J Exp Biol 131:117–135.

Felts WJL. 1966. Some functional and structural characteristics of cetacean flippers and flukes. In: Norris KS, editor. Whales, dolphins, and porpoises. Berkeley (CA): University of California Press. p. 255–276.

Fish FE. 1993a. Influence of hydrodynamic design and propulsive mode on mammalian swimming energetics. Aust J Zool 42:79–101.

Fish FE. 1993b. Power output and propulsive efficiency of swimming bottlenose dolphins (*Tursiops truncatus*). J Exp Biol 185:179–193.

Fish FE. 1996. Transitions from drag-based to lift-based propulsion in mammalian aquatic swimming. Am Zool 36:628–641.

Fish FE. 1998a. Comparative kinematics and hydrodynamics of odontocete cetaceans: morphological and ecological correlates with swimming performance. J Exp Biol 201:2867–2877.

Fish FE. 1998b. Biomechanical perspective on the origin of cetacean flukes. In: Thewissen JGM, editor. The emergence of whales: evolutionary patterns in the origin of Cetacea. New York: Plenum Press. p. 303–324.

Fish FE. 2002. Balancing requirements for stability and maneuverability in cetaceans. Integr Comp Biol 42:85–93.

Fish FE. 2006a. Limits of nature and advances of technology in marine systems: what does biomimetics have to offer to aquatic robots? Appl Bionics Biomech 3:49–60.

Fish FE. 2006b. The myth and reality of Gray's paradox: implication of dolphin drag reduction for technology. Bioinspir Biomim 1:R17–R25.

Fish FE, Battle JM. 1995. Hydrodynamic design of the humpback whale flipper. J Morph 225:51–60.

Fish FE, Hui CA. 1991. Dolphin swimming - a review. Mamm Rev 21:181–195.

Fish FE, Innes S, Ronald K. 1988. Kinematics and estimated thrust production of swimming harp and ringed seals. J Exp Biol 137:157–173.

Fish FE, Lauder GV. 2006. Passive and active flow control by swimming fishes and mammals. Annu Rev Fluid Mech 38:193–224.

Fish FE, Nicastro AJ, Weihs D. 2006b. Dynamics of the aerial maneuvers of spinner dolphins. J Exp Biol 209:590–598.

Fish FE, Nusbaum MK, Beneski JT, Ketten DR. 2006a. Passive cambering and flexible propulsors: cetacean flukes. Bioinspir Biomim 1:S42–S48.

Fish FE, Rohr J. 1999. Review of dolphin hydrodynamics and swimming performance. San Diego (CA): SPAWARS System Center Technical Report 1801.

Gertler M. 1950. Resistance experiments on a systematic series of streamlined bodies of revolution-for application to the design of high-speed submarines. Washington (DC): Rep C-297, David W. Taylor Model Basin.

Gray J. 1936. Studies in animal locomotion VI. The propulsive powers of the dolphin. J Exp Biol 13: 192–199.

Hain JHW, Carter GR, Kraus SD, Mayo CA, Winn HE. 1982. Feeding behavior of the humpback whale, *Megaptera novaeangliae*, in the western North Atlantic. Fish Bull 80:259–268.

Hanke W, Brücker C, Bleckman H. 2000. The aging of the low-frequency water disturbances caused by swimming goldfish and its possible relevance to prey detection. J Exp Biol 203:1193–1200.

Hertel H. 1966. Structure, form and movement. New York: Rheinhold.

Hoerner SF. 1965. Fluid-dynamic drag. Brick Town (NJ): Published by author.

Howell AB. 1930. Aquatic mammals. Springfield (IL): Charles C. Thomas.

Hurt HH, Jr. 1965. Aerodynamics for naval aviators. U.S. Navy, NAVWEPS 00-80T-80.

Iosilevskii G, Weihs D. 2007. Speed limits to swimming of fishes and cetaceans. J R Soc Interface. doi 10.1098/rsif.2007.1073.2007.

Johari H, Henoch C, Custodio D, Levshin A. 2007. Effects of leading-edge protuberances on airfoil performance. AIAA J 45:2634–2642.

Jurasz CM, Jurasz VP. 1979. Feeding modes of the humpback whale, *Megaptera novaeangliae*, in southeast Alaska. Sci Rep Whales Res Inst 31:69–83.

Katz J, Weihs D. 1978. Hydrodynamic propulsion by large amplitude oscillation of an airfoil with chordwise flexibility. J Fluid Mech 88:485–497.

Katz J, Weihs D. 1979. Large amplitude unsteady motion of a flexible slender propulsor. J Fluid Mech 90:713–723.

Kojeszewski T, Fish FE. 2007. Swimming kinematics of the Florida manatee (*Trichechus manatus latirostris*): hydrodynamic analysis of an undulatory mammalian swimmer. J Exp Biol 210:2411–2418.

Lang T G. 1966. Hydrodynamic analysis of cetacean performance. In: Norris KS, editor. Whales, dolphins and porpoises. Berkeley (CA): University. of California Press. p. 410–432.

Lang TG. 1975. Speed, power, and drag measurements of dolphins and porpoises. In: Wu TY, Brokaw CJ, Brennen C, editors. Swimming and flying in nature. New York: Plenum Press. p. 553–571.

Lang TG, Daybell DA. 1963. Porpoise performance tests in a seawater tank. China Lake, CA: Nav Ord Test Sta Tech Rep. p. 3063.

Liao JC. 2004. Neuromuscular control of trout swimming in a vortex street: implications for energy economy during the Kámán gait. J Exp Biol. 207:3495–3506.

Lighthill J. 1969. Hydrodynamics of aquatic animal propulsion - a survey. Annu Rev Fluid Mech 1:413–446.

Lighthill J. 1975. Mathematical biofluiddynamics. Philadelphia (PA): Society for Industrial and Applied Mathematics.

Lindsey CC. 1978. Form, function, and locomotory habits in fish. In: Hoar WS, Randall DJ, editors. Fish physiology: locomotion, Vol. 7. New York: Academic Press. p. 1–100.

Liu P, Bose N. 1993. Propulsive performance of three naturally occurring oscillating propeller planforms. Ocean Eng 20:57–75.

Long JH Jr, Pabst DA, Shepherd WR, McLellan WA. 1997. Locomotor design of dolphin vertebral columns: bending mechanics and morphology of *Delphinus delphis*. J Exp Biol 200:65–81.

Miklosovic DS, Murray MM, Howle LE. 2007. Experimental evaluation of sinusoidal leading edges. J Aircr 44: 1404–1407.

Miklosovic DS, Murray MM, Howle LE, Fish FE. 2004. Leading edge tubercles delay stall on humpback whale (*Megaptera novaeangliae*) flippers. Phys Fluids 16:L39–L42.

Moin P, Kim J. 1997. Tackling turbulence with supercomputers. Sci Am 276:62–68.

Owen JC, Szewczyk AA, Bearman PW. 2000. Suppression of Karman vortex shedding. Phys Fluids 12:S9.

Pabst DA. 1996. Springs in swimming animals. Am Zool 36:723–735.

Parry DA. 1949. The swimming of whales and a discussion of Gray's paradox. J Exp Biol 26:24–34.

Paterson EG, Wilson RV, Stern F. 2003. General-purpose parallel unsteady RANS CFD code for ship hydrodynamics. IIHR Hydroscience and Engineering Report 531. Iowa City (IA): The University of Iowa.

Pauly D, Trites AW, Capuli E, Christensen V. 1998. Diet composition and trophic levels of marine mammals. Mar Mamm Sci 55:467–481.

Pavlov VV. 2006. Dolphin skin as a natural anisotropic compliant wall. Bioinspir Biomim 1:31–40.

Pilleri G, Peixun C. 1979. How the finless porpoise (*Neophocaena asiaeorientalis*) carries its calves on its back, and the function of the denticulated area of skin, as observed in the Changjiang River, China. Invest Cetacea 10:105–110.

Prandtl L, Tietjens OG. 1934. Applied hydro- and aeromechanics. New York: Dover.

Prempraneerach P, Hover FS, Triantafyllou MS. 2003. The effect of chordwise flexibility on the thrust and efficiency of a flapping foil. 13th International Symposium on Unmanned Submersible Technology. Durham (NC): Autonomous Undersea Institute.

Renouf D. 1979. Preliminary measurements of the sensitivity of the vibrissae of Harbour seals (*Phoca vitulina*) to low frequency vibrations. J Zool (Lond) 188:443–450.

Ridgway SH, Harrison R. 1985. Handbook of marine mammals vol. 3: the sirenians and baleen whales. London: Academic Press.

Ridgway SH, Harrison R. 1999. Handbook of marine mammals vol. 5: river dolphins and the larger toothed whales. London: Academic Press.

Rohr J, Latz MI, Fallon S, Nauen JC, Hendricks E. 1998. Experimental approaches towards interpreting dolphin-stimulated bioluminescence. J Exp Biol 201:1447–1460.

Rohr JJ, Fish FE. 2004. Strouhal numbers and optimization of swimming by odontocete cetaceans. J Exp Biol 207:1633–1642.

Rohr JJ, Fish FE, Gilpatrick JW. 2002. Maximum swim speeds of captive and free ranging delphinids: critical analysis of extraordinary performance. Mar Mamm Sci 18:1–19.

Romanenko EV. 2002. Fish and dolphin swimming. Sofia: Pensoft.

Saunders HE. 1957. Hydrodynamics in ship design. New York: Soc Nav Arch Mar Eng.

Taubes G. 2000. Biologists and engineers create a new generation of robots that imitate life. Science 288:80–83.

Taylor G, Wang Z, Vardaki E, Gursul I. 2007. Lift enhancement over flexible nonslender delta wings. AIAA J 45:2979–2993.

Tomilin AG. 1957. Mammals of the U.S.S.R. and adjacent countries. vol. 9: Cetacea. Moscow: Nauk S.S.S.R. (English Translation, 1967, Israel Program for Scientific Translations, Jerusalem).

Triantafyllou GS, Triantafyllou MS. 1995. An efficient swimming machine. Sci Am 272:40–48.

True FW. 1983. The whalebone whales of the western North Atlantic. Washington, DC: Smithsonian Institution Press.

van Nierop EA, Alben S, Brenner MP. 2008. How bumps on whale flippers delay stall: an aerodynamic model. Phys Rev Lett. 100:054502.

Vogel S. 1994. Life in moving fluids. Princeton (NJ): Princeton University Press.

Vogel S. 1998. Cat's paws and catapults. New York: WW Norton.

von Mises R. 1945. Theory of flight. New York: Dover.

Walsh MJ. 1990. Riblets. Prog Astro Aero 123:203–261.

Watts P, Fish FE. 2001. The influence of passive, leading edge tubercles on wing performance. Proceedings of the Twelfth International Symposium on Unmanned Untethered Submersible Technology. Durham (NC): Autonomous Undersea Systems Institute.

Webb PW. 1975. Hydrodynamics and energetics of fish propulsion. Bull Fish Res Bd Can 190:1–158.

Webb PW. 1978. Hydrodynamics: Nonscombrid fish. In: Hoar WS, Randall DJ, editors. Fish physiology: Locomotion, vol. 7. New York: Academic Press. p. 189–237.

Weihs D. 1972. Semi-infinite vortex trails, and their relation to oscillating airfoils. J Fluid Mech 54:679–690.

Weihs D. 1981. Effects of swimming path curvature on the energetics of fish swimming. Fish Bull 79:171–176.

Weihs D. 1993. Stability of aquatic animal locomotion. Cont Math 141:443–461.

Whitehead H, Carlson C. 1988. Social behaviour of feeding finback whales off Newfoundland: comparisons with the sympatric humpback whale. Can J Zool 66:217–221.

Williams TM. 1998. The evolution of cost efficient swimming in marine mammals: limits to energetic optimization. Philos Trans R Soc Lond B Biol Sci 353:1–9.

Winn HE, Reichley NE. 1985. Humpback whale *Megaptera novaeangliae* (Borowski, 1781). In: Ridgway SH, Harrison R, editors. Handbook of marine mammals, vol. 3: The sirenians and baleen whales. London: Academic Press. p. 241–273.

Wolfgang MJ, Anderson JM, Grosenbaugh MA, Yue DKP, Triantafyllou MS. 1999. Near-body flow dynamics in swimming fish. J Exp Biol 202:2303–2327.

Woodward BL, Winn JP, Fish FE. 2006. Morphological specialization of baleen whales according to ecological niche. J Morph 267:1284–1294.

Wu JZ, Vakili AD, Wu JM. 1991. Review of the physics of enhancing vortex lift by unsteady excitation. Prog Aerospa Sci 28:73–131.

Wu TY. 1971. Hydromechanics of swimming fishes and cetaceans. Adv Appl Mech 11:1–63.